

# ANALYSIS OF ADIABATIC TRAPPING FOR QUASI-INTEGRABLE AREA-PRESERVING MAPS

Armando Bazzani\*

*Physics and Astronomy Department,  
Bologna University, V. Irnerio 46, Bologna - IT*

Christopher Frye†

*Departments of Physics and Mathematics,  
University of Central Florida, Orlando, Florida - US and  
Beams Department, CERN, 1211 Genève 23 - CH*

Massimo Giovannozzi‡

*Beams Department, CERN, 1211 Genève 23 - CH*

Cédric Hernalsteens§

*Beams Department, CERN, 1211 Genève 23 - CH and  
EPFL, LPAP, CH-1015 Lausanne - CH*

(Dated: February 5, 2014)

## Abstract

Trapping phenomena involving non-linear resonances have been considered in the past in the framework of adiabatic theory. Several results are known for continuous-time dynamical systems generated by Hamiltonian flows in which the combined effect of non-linear resonances and slow time-variation of some system parameters are considered. The focus of this paper is on discrete-time dynamical systems generated by two-dimensional symplectic maps. The possibility of extending the results of neo-adiabatic theory to quasi-integrable area-preserving maps is discussed. Scaling laws are derived, which describe the adiabatic transport as a function of the system parameters using a probabilistic point of view. These laws can be particularly relevant for physical applications. The outcome of extensive numerical simulations showing the excellent agreement with the analytical estimates and scaling laws is presented and discussed in detail.

PACS numbers: 05.45.-a, 45.10.Hj, 45.20.Jj

---

\* armando.bazzani@bo.infn.it

† christopher.frye@knights.ucf.edu

‡ massimo.giovanozzi@cern.ch

§ cedric.hernalsteens@cern.ch

## I. INTRODUCTION

The neo-adiabatic theory [1–6] has been developed to estimate the change of the adiabatic invariant when separatrix crossing phenomena occur in slowly modulated one-degree of freedom Hamiltonian systems. The theory provides explicit formulæ for the trapping probabilities into a resonance region [2], for the change of the adiabatic invariant due to separatrix crossing, and for the error estimate defining the regions of validity in phase space [3].

Adiabatic transport is also possible under these conditions. In fact, an ensemble of particles trapped into a resonance region can be moved at a distance of order  $O(1)$  in a time  $O(1/\epsilon)$ , where  $\epsilon$  is the adiabatic parameter that defines the slow time scale. The adiabatic transport by means of non-linear resonances has relevant applications in plasma physics [7, 8], accelerator physics [9–12], celestial mechanics [13–15], and in general for controlling a particle distribution under the effect of non-linear dynamics. It is also worth mentioning that even if plasma and accelerator physics are the typical domains of applicability of adiabatic theory, fields as diverse as quantum systems, nanostructures, and superconductors are also dealing with problems of adiabatic transport (see, e.g., Refs. [16–18]).

The application of the theoretical results to physical experiments has to face the problem of a quantitative evaluation of the theory’s limits and of the extension of the analytical results to realistic models. [In many situations the theory suggests the existence of simple relations among physical observables, which can be extended to very generic situations due to their robustness character. According to this remark,](#) we perform analytical and numerical studies to derive scaling laws for the efficiency of the adiabatic trapping and transport in quasi-integrable Hamiltonian systems. In particular we consider the possibility to extend the neo-adiabatic theory to analytic area-preserving maps in a neighbourhood of an elliptic fixed point, for which, to our best knowledge, no rigorous result exists, yet.

The numerical simulations show that such scaling laws are robust and they apply to a wide class of models even if a rigorous extension of the neo-adiabatic invariance theory is not possible, due to the presence of infinite non-linear resonances in phase space [19, 20].

This is the case of quasi-integrable systems like the Hénon map [21], which is a relevant model to study non-linear effects in celestial mechanics and accelerator physics [22]. To cope with the problem of non-integrability we take advantage of the existence of a *interpolating Hamiltonian* (i.e. an Hamiltonian whose phase flux interpolates at integer times the

orbits of the maps) in a neighbourhood of the elliptic fixed point with an error that can be exponentially small in the distance from the elliptic fixed point [23].

The interpolating Hamiltonian can be perturbatively computed using the Birkhoff Normal Forms [22, 24, 25]. To extend partially the neo-adiabatic theory to area-preserving maps we have to consider the effect of the discrete time dependence which implies the existence of an infinite number of resonances in the phase space. [In this paper it is shown that the formulæ for continuous-time can also be applied to discrete-time systems, as long as the definition of the improved adiabatic invariant \(IAI\) is modified to control the dynamics near the separatrix curve, which requires a cut-off in the Fourier expansion in the action-angle variables to be introduced. Moreover, thanks to the theoretical considerations outlined here, which set a rigorous framework for the analysis of discrete time systems, it is possible to compute explicitly the dependence of the trapping efficiency from the adiabatic parameter and the characteristics of the resonance under consideration.](#)

It is worth mentioning that numerical simulations on slowly modulated Hamiltonian systems have been performed by various authors mainly to study the weak chaotic regions swept by a moving resonance and the diffusion behaviour of the orbits in phase space [26–28]. In this paper, however, we adopt a different [and original point of view](#). On one side we use numerical simulations to study the limits of the theoretical results, which require specific conditions on the adiabatic parameters and the resonance structure. Also, we aim at evaluating the efficiency of adiabatic transport under different situations relevant for applications. On another side, the numerical simulations allow to define specific protocols of time-variation of the free parameters of the system under consideration, in view of optimising the adiabatic transport according to specific requirements, e.g., the control of final particle distribution in phase space such as in Refs. [29–31]. [It is worth stressing that the points addressed in this paper are extremely relevant in applications. In particular, in the field of beam physics, where crossing a non-linear resonance has been proposed as a means to split the beam in the transverse phase space \[9–12\] to perform a multi-turn extraction from a circular particle accelerator. This novel technique requires an accurate control of the intensity sharing between the various beamlets as well as of the losses during transport of the trapped beamlets. Therefore, theoretical and robust scaling laws describing the detail of the trapping process are essential for optimising the actual beam manipulation.](#)

The plan of the paper is as follows: in section II some results of the neo-adiabatic the-

ory for Hamiltonian flows are presented and extended to discrete-time systems (maps) as required for our study. The analysis of pendulum-like systems is presented in section III, discussing the details of the trapping process, its optimisation, and the efficiency of transport of the trapped initial conditions. Analytical area-preserving maps, a generalisation of the Hénon map, are dealt with in section IV, where the details of the trapping process are studied, with particular emphasis on the dependence of the fraction of trapped orbits on the distribution of initial conditions and on the system's parameters. Furthermore, scaling laws for phase space area around the origin where trapping into resonance cannot occur are also presented and discussed in detail. Finally, some conclusions are drawn in section V, [and in Appendix A a number of results that are used in the main body of the paper are collected.](#)

## II. ADIABATIC THEORY AND TRAPPING INTO RESONANCE

### A. Adiabatic theory for quasi-integrable area-preserving maps

The extension of adiabatic theory to area-preserving maps has to address a number of specific issues due to the discontinuous nature of their time dependence. Indeed if one considers a slowly modulated area-preserving map written in the form

$$(q_{n+1}, p_{n+1}) = \mathcal{M}(q_n, p_n, \epsilon n) \quad \epsilon \ll 1 \quad (1)$$

a discontinuous change in the dynamics occurs at each iteration. Letting  $\lambda = \epsilon n$  we initially assume that the *frozen map* is integrable, so that there exists an Hamiltonian  $H(q, p, \lambda)$  such that

$$\mathcal{M}(q, p, \lambda) = \exp[D_{H(q,p,\lambda)}](q, p) \quad (2)$$

where the operator  $D_{H(q,p,\lambda)}$  is the Lie derivative defined using the Poisson Bracket  $[\cdot, \cdot]$  as

$$D_{H(q,p,\lambda)}f(q, p) = [f(q, p), H(q, p, \lambda)] = \sum_i \frac{\partial f}{\partial q_i} \frac{\partial H}{\partial p_i} - \frac{\partial f}{\partial p_i} \frac{\partial H}{\partial q_i}.$$

As a consequence  $H(q, p, \epsilon t)$  is an *interpolating Hamiltonian* for the map (1) with an error of order  $O(\epsilon)$ : i.e., the phase flow associated with  $H(q, p, \epsilon t)$  interpolates the orbits  $(q_n, p_n)$  up to an error  $O(\epsilon)$ . This fact prevents the possibility of applying directly the results of adiabatic theory for Hamiltonian systems to the modulated map (1). [Indeed, in Appendix A we show how the existence of an interpolating Hamiltonian allows extending the adiabatic](#)

theory to maps of type (1) under suitable conditions. Using perturbation theory it is in fact possible to introduce action-angle variables  $(\phi, J)$  such that the modulated map

$$\mathcal{M}(\theta_n, I_n, \lambda) = \exp[\epsilon D_{\partial F/\partial \lambda}(\theta_n, I_n, \lambda)] \exp[D_{H(I_n, \lambda)}](\theta_n, I_n) + O(\epsilon^2) \quad \lambda = \epsilon n \quad (3)$$

can be written in the form

$$\phi_{n+1} = \phi_n + \Omega(J_n, \phi_n, n\epsilon) + O(\epsilon^2) \quad (4)$$

$$J_{n+1} = J_n + O(\epsilon^2)$$

provided no resonances

$$k \Omega(I, \lambda) = 2 \pi h \quad h \in \mathbb{Z} \quad (5)$$

are present in the phase space region under consideration, taking also into account the values spanned by varying  $\lambda$ , provided  $|k| \leq k_{\max}$ , where  $k_{\max}$  is an appropriate cut-off (see Appendix A).

To control the evolution of the adiabatic invariant up to the separatrix we have to show that the cut-off error does not depend on the distance to the separatrix curve. This is indeed the case according to the results reported in Appendix A.

In section IV we show, using numerical simulations, that the previous results can be extended to area-preserving maps in a neighbourhood of an elliptic fixed point. Indeed in this case the Birkhoff Normal Forms theory suggests the existence of an interpolating Hamiltonian for the frozen map in a neighbourhood of the of the elliptic point, whose error becomes exponentially small  $\propto \exp[-(r_0/r)^\eta]$  when approaching the elliptic fixed point ( $r \rightarrow 0$ ) [23] where  $r_0, \eta$  are suitable positive constants depending from the arithmetic property of the linear frequency. Even if the explicit calculation of the optimal interpolating Hamiltonian is not possible, the perturbative approach based on Birkhoff Normal Forms allows to point the dependence of the phase space structure from the map parameters. Therefore according to the previous assumptions, by considering the neighbourhood of the origin where the error is  $O(\epsilon^3)$ , we can prove the existence of an IAI for the modulated map.

## B. Trapping into resonance and change of adiabatic invariant when crossing a separatrix

According to the Birkhoff Normal Forms, the interpolating Hamiltonian for an analytic area-preserving map in a neighbourhood of an elliptic fixed point can be written in the form [22]

$$H(\rho, \psi, \lambda) = H_0(\rho, \lambda) + A(\lambda) \rho^{m/2} \cos m\psi + O(\rho^{m+1}) \quad (6)$$

where  $m$  is the considered resonance order and

$$\rho = \frac{q^2 + p^2}{2} \quad \psi = \text{atan} \frac{q}{p}. \quad (7)$$

Without loss of generality we assume that

$$H_0(\rho, \lambda) \simeq \omega_1(\lambda) \rho + \frac{\omega_2(\lambda)}{2} \rho^{\hat{m}} \quad (8)$$

where  $\omega_2(\lambda) < 0$  and  $\omega_1(\lambda)$  is a monotonic function, satisfying  $\omega_1 \in [-\delta, \delta]$  when  $\lambda \in [0, 1]$ . If  $\hat{m} < m$  then the resonance is stable; otherwise it is unstable, as the separatrices can pass through the origin. Most of the computations reported in this paper refer to  $m = 4$  and  $\hat{m} = 2$ .

A scaling argument on Hamiltonian systems of the form (6) suggests that the parameter  $\gamma_0$  of Eq. (A21) is expected to be of order  $1/\delta$ , so that if  $\delta$  is small enough we can apply the adiabatic theory to the time-dependent map, as  $\epsilon$  can be chosen small.

The existence of real, positive solutions in  $\rho$  to the equation  $\partial H_0/\partial \rho = 0$  for fixed  $\lambda$  implies the existence of separatrix curves for the frozen system and we distinguish three different regions in phase space (see also Fig.1, left):

- the region above the resonance islands (Region *I*);
- the region below the resonance islands (Region *II*);
- the region inside the resonance islands (Region *III*).

According to the remarks in the previous section and in Appendix A, we can compute an IAI for an adiabatically modulated maps in the form

$$J = I + \frac{\epsilon}{2\pi} \int_0^{\mathcal{T}} \left( \frac{\mathcal{T}}{2} - t \right) \mathbb{T}_\Omega \left\{ \frac{\partial H}{\partial \lambda} \right\}_{\leq k_{\max}(\Omega(I, \lambda), \epsilon)} dt \quad (9)$$

where  $\mathcal{T}(I, \lambda)$  is the orbit period of the frozen system, and  $\{\cdot\}_k$  stands for the truncation of the Fourier expansion to order  $k$ , using the same approach as for Hamiltonian systems. The change of the adiabatic invariant due to separatrix crossing is estimated applying Neishtadt's theory [3], since since the IAI (9) tends to the IAI of the interpolating Hamiltonian. Moreover, the evolution of the frozen energy  $H(\rho, \psi, \lambda) = E$  and of the scaled period  $\epsilon \mathcal{T}(J, \lambda)$  can be described by the interpolating Hamiltonian dynamics up to an error  $O(\epsilon^2)$ .

We are interested in describing the time-evolution of an ensemble of particles initially distributed in Region *I* of phase space under the effect of surface increase, induced by the change of parameter  $\lambda$ , of both Regions *II* and *III*. Following Neishtadt, we consider the phase space areas  $\Sigma_{II,III}(\lambda)$  enclosed by the separatrix curves in Regions *II* and *III*, which are both bounded, and we define

$$\Sigma_I = \Sigma_{II} + \Sigma_{III} \quad , \quad \frac{d\Sigma_i}{d\lambda} = \Theta_i(\lambda) > 0 \quad i = I, II, III; \quad (10)$$

then  $\Theta_I = \Theta_{II} + \Theta_{III}$  represents also the derivative of the surface of Region *I*, but with opposite sign. **The condition  $\Theta_{II,III} > 0$  is mandatory to have a non-zero trapping probability in Regions II and III, as they are growing during the resonance crossing process.**

For each particle, we introduce the so-called crossing parameter  $\lambda_*$  according to the equation  $\Sigma_I(\lambda_*) = 2\pi J_-$  where  $J_-$  is the initial value of the invariant  $J$  in Region *I*. The existence of the crossing parameter implies that the particle can enter into either Region *II* or *III* by the effect of the separatrix crossing.

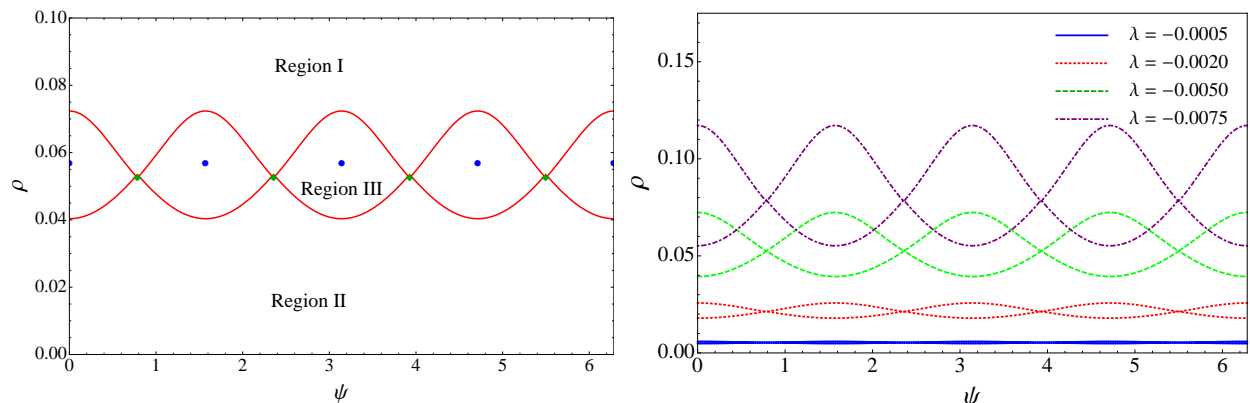


FIG. 1. Schematic view of the regions generated by the separatrix of the frozen system (6) (left) and position of the separatrix for the same system, but including the  $\lambda$ -dependence (right).

When the adiabatic theory holds, it is possible to prove that the transition probability



from Region  $I$  to Regions  $II$  and  $III$  is given by

$$P_{I \rightarrow II} = \frac{\Theta_{II}}{\Theta_I} \quad P_{I \rightarrow III} = \frac{\Theta_{III}}{\Theta_I}. \quad (11)$$

The transition phenomenon induced by the separatrix crossing is described in a probabilistic way [32] by using the random variables

$$\xi_I = \frac{|h_0^I|}{\epsilon \Theta_I} \quad \xi_{II} = \frac{|h_0^{II}|}{\epsilon \Theta_{II}} \quad (12)$$

where  $h_0^I$  and  $h_0^{II}$  are the orbit energy computed via the interpolating Hamiltonian, at Poincaré sections of phase space just before entering into Region  $III$  or just after entering into Region  $II$ , respectively. It turns out that the variables  $\xi_i$  are uniformly distributed in the interval  $[0, 1]$  and they are quite sensitive to the value of  $J_-$ . Moreover, the theory is correctly applied only when  $K \sqrt{\epsilon} < \xi_i < 1 - K \sqrt{\epsilon}$  for a suitable positive constant  $K$ . This condition allows an easy estimate of the fraction of particles whose evolution is not described by the adiabatic theory. Once the separatrix crossing phenomenon occurs, one can compute the change of the IAI in the new phase space region. For the transition  $I \rightarrow III$  in a generic case we have the estimate

$$2\pi J_+ - \Sigma_{III}(\lambda_*) = -\epsilon \alpha \Theta_{III} \left( \xi_I - \frac{1}{2} \right) \left( \ln \epsilon \Theta_I - \frac{2\Theta_I}{\Theta_{III}} \ln \epsilon \Theta_{III} \right) + O(\epsilon) \quad (13)$$

where  $J_+$  is the final value of the IAI, while  $\alpha$  is the inverse of the logarithm of the eigenvalue of the frozen map at the hyperbolic fixed point. Similarly the transition  $I \rightarrow II$  gives a change in the IAI of

$$2\pi J_+ - \Sigma_{II}(\lambda_*) = -\epsilon \alpha \Theta_{II} (\xi_{II} - 1) \left( \ln \epsilon \Theta_I + \frac{\Theta_I}{\Theta_{II}} \ln \epsilon \Theta_{II} \right) + O(\epsilon). \quad (14)$$

In the previous estimates we have only reported the leading terms of order  $O(\epsilon \ln \epsilon)$  in a generic system (for a more detailed result see Refs. [3, 26]) since our goal is to describe the adiabatic trapping into resonance region for an ensemble of particles. Referring to the phase space structure of the Hamiltonian (6), we assume that when the parameter  $\lambda$  is varied, the resonance region is enlarged and moved outwards (see Fig. 1, right). As a consequence the areas of Regions  $II$  and  $III$  increase and an orbit starting in Region  $I$  can be trapped in Regions  $II$  or  $III$  provided that adiabatic theory applies. An orbit starting in Region  $I$  tends to preserve the IAI value during the slow variation of  $\lambda$  until it reaches the separatrix when  $\lambda = \lambda_*$ . Then, it is possible to describe the separatrix crossing phenomenon if the

orbit is not too close to the hyperbolic point (condition on the  $\xi_i$  variables) neglecting terms of order  $O(\epsilon^{3/2})$  and the IAI performs a pseudo-stochastic dynamics according to Eqs. (13) and (14).

Some conditions need to be fulfilled for the adiabatic theory to be applicable. For the Hamiltonian (6) we define the adiabatic parameter  $\varepsilon$  as the ratio between  $\epsilon$  and the square of the secondary frequency  $\omega_e^2$ , *i.e.*, [the frequency of small oscillations around the elliptic fixed point inside the resonance region](#). When the adiabatic parameter  $\varepsilon$  is  $O(1)$  one cannot justify the estimates (13) and (14). Consequently we lose the control of the adiabatic invariant at the separatrix crossing and the adiabatic trapping into resonances is not possible. When the resonance is stable and  $\omega_1 \ll \omega_2$  (see Eq. (8)), a perturbative approach [22] applied to the Hamiltonian (6) provides the estimates for the frequency of the elliptic fixed points

$$\omega_e^2 \simeq \frac{A}{\omega_2} \left( \frac{\omega_1}{\omega_2} \right)^{m/2}$$

whereas the resonance distance from the origin is

$$r_e \propto \sqrt{\frac{\omega_1}{\omega_2}}.$$

Then the smallness condition on the adiabatic parameter reads

$$\varepsilon = \frac{\epsilon}{\omega_e^2} \propto \frac{\epsilon \omega_2}{r_e^m} \ll 1 \quad \Rightarrow \quad \epsilon \ll \frac{r_e^m}{\omega_2} \quad (15)$$

and we derive the following scaling law for the minimum distance of the resonance from the origin which allows the trapping phenomenon to start (*trapping radius*):

$$R_{\min} \propto \epsilon^{1/m}. \quad (16)$$

In a similar way one can prove that if the condition (15) holds, then the change of the IAI is small compared to the area of the resonance Region *III*, which also scales as  $r_e^{m/2}(\lambda)$  for the Hamiltonian (6).

The situation changes in the case of unstable resonances. As an example, we consider the third order resonance ( $m = 3$ ), for which the interpolating Hamiltonian is approximated by

$$H \simeq -\omega_1 \rho - A \rho^{3/2} \cos 3\theta + \omega_2 \frac{\rho^2}{2}$$

and the hyperbolic fixed points are located at  $\theta_c = \pi/3$  and at a distance

$$r_c = -\frac{3A}{4\omega_2} + \sqrt{\left(\frac{3A}{4\omega_2}\right)^2 + \frac{\omega_1}{\omega_2}} \simeq \frac{2\omega_1}{3A}$$

so that  $r_c \propto \omega_1$ , which is the frequency of the elliptic fixed point at the origin. The condition on the adiabatic parameter reads

$$\frac{\epsilon}{\omega_1^2} \ll 1$$

and the radius  $r_c$  satisfies the scaling law

$$\frac{\epsilon}{r_c^2} \ll 1 \quad \Rightarrow \quad R_{\min} \propto \epsilon^{1/2}. \quad (17)$$

For a generic unstable resonance of order  $m$  we can perform similar calculations obtaining a scaling law for the minimum radius

$$R_{\min} \propto \epsilon^{1/2(m-2)}. \quad (18)$$

The trapping efficiency can be evaluated considering that the theory applies to the orbits which do not pass too close to the hyperbolic fixed points (i.e.,  $\xi_i \in [K\sqrt{\epsilon}, 1 - K\sqrt{\epsilon}]$ ). Therefore, whenever  $\Theta_{III} > 0$  the trapping efficiency is given by

$$c_{I \rightarrow III}(\lambda) = \frac{\Theta_{III}(\lambda)}{\Theta_I(\lambda)} (1 - 2K\sqrt{\epsilon}). \quad (19)$$

Letting  $n(\rho)$  be the radial density of the ensemble of particles, then the total number of trapped particles will be given by

$$N_{III} = \int_{\lambda_0}^{\lambda_1} n(\rho(\lambda)) \frac{\Theta_{III}(\lambda)}{\Theta_I(\lambda)} \left[ 1 - 2K \frac{\sqrt{\epsilon}}{\omega_e(\lambda)} \right] d\lambda \quad (20)$$

and we have the relation

$$N_{III} = c_0 - c_1 \sqrt{\epsilon} = c_0 - c_1 \sqrt{\frac{|\lambda_1 - \lambda_0|}{T}} \quad (21)$$

where  $T = |\lambda_1 - \lambda_0|/\epsilon$  is the time interval over which the trapping process takes place. It is worth stressing that indeed the lower limit of integration  $\lambda_0$  might need to be replaced by  $\min(\lambda_0, R_{\min})$  to take into account the loss of adiabaticity close to the origin of phase space. This phenomenon occurs also for the particles that enter into Region *II* from Region *I*. In fact, a fraction proportional to

$$c_{I \rightarrow II}(\lambda) = \frac{\Theta_{II}(\lambda)}{\Theta_I(\lambda)} (1 - 2K\sqrt{\epsilon}) \quad (22)$$

changes the IAI according to the theory, whereas the other particles may be scattered in phase space [14].

The particles not trapped may feature a large variation in the adiabatic invariant, thus changing the particles' distribution in phase space. This point is essential for our considerations. In fact, if the initial distribution is strongly affected by the change of IAI during the crossing process, then the estimate given in Eq. (20) (and similarly for  $N_{II}$ ) is no longer correct, as  $n(\rho)$  should account also for the dynamical change of shape during the resonance crossing process.

### III. ADIABATIC TRANSPORT FOR PENDULUM-LIKE SYSTEMS

In order to study the parametric dependence of the adiabatic transport in this section we consider pendulum-like Hamiltonian systems whose Hamiltonian function has the form

$$H(\theta, I, \lambda) = \frac{1}{2} [I - \delta(\lambda)]^2 - [1 + \beta(\lambda)] \cos \theta, \quad (23)$$

where  $\delta, \beta$  are functions with  $\beta(\lambda) > -1$ . This Hamiltonian has been also considered in Ref. [33] to study transport due to resonance trapping. The expression for the fixed points is given by

$$I = \delta(\lambda) \quad \text{and} \quad \theta = n\pi \text{ with integer } n \quad (24)$$

and it is easy to find that for  $n = 0$  the fixed point is elliptic (or stable), while for  $n = 1$  it is hyperbolic (or unstable). The equation of the separatrix emanating from the hyperbolic fixed point reads

$$I_{\pm}^*(\lambda, \theta) = \delta(\lambda) \pm 2 \cos\left(\frac{\theta}{2}\right) \sqrt{1 + \beta(\lambda)}, \quad (25)$$

while the area of the stable island and its  $\lambda$ -derivative is given by

$$\Sigma_{III} = 16 \sqrt{1 + \beta(\lambda)} \quad \Theta_{III} = \frac{8 \dot{\beta}(\lambda)}{\sqrt{1 + \beta(\lambda)}}. \quad (26)$$

The last quantity that is relevant for our analysis is the angular frequency of oscillation around the elliptic fixed point, which is equal to

$$\omega_e(\lambda) = \sqrt{1 + \beta(\lambda)}. \quad (27)$$

The meaning of the auxiliary functions  $\delta$  and  $\beta$  is clear:  $\delta(\lambda)$  represents the shift along the  $I$ -axis of the fixed point, while  $\beta(\lambda)$  is related with the size of the stable island. Therefore, these two parameters allow controlling the resonance position and size in an independent

way. This is an essential feature of this model, which enables an optimal control of the global dynamics to allow an accurate assessment of the impact of the island growth and transport on the trapping phenomenon. Unfortunately, such an independent control is lost in the case of the area-preserving maps that will be considered in section IV.

### A. Analysis of trapping efficiency

To illustrate the analytic results and their predictive power we consider a rather complex variation of the free parameters of the pendulum-like system in order to mimic what could be an optimised trapping and transport process. A uniform initial distribution of particles given by

$$n(\theta, I) = \begin{cases} N/2\pi & \text{for } (\theta, I) \in [-\pi, \pi] \times [0, 1] \\ 0 & \text{otherwise} \end{cases} \quad (28)$$

has been used in the numerical simulations. We will also let  $\delta$  increase linearly from  $\delta(0) = 0.5$  to  $\delta(1) = 1.5$  during a time  $T = 1/\epsilon$ , where  $\lambda = \epsilon t = t/T$ , and

$$\delta(\lambda) = \frac{1}{2} + \lambda. \quad (29)$$

Furthermore,  $\beta$  will increase quadratically from  $\beta(0) = \beta_i$  (if  $\beta_i = -1$  the stable island begins as a slit with zero size at the centre of the initial conditions) to some  $\beta(1) = \beta_f$  which we keep arbitrary for now:

$$\beta(\lambda) = (\beta_f - \beta_i)\lambda^2 + \beta_i. \quad (30)$$

A key quantity that will be considered throughout this paper is the so-called trapping fraction  $\tau$ , which is defined as the ratio between the initial conditions that are trapped into the non-linear resonance and the total number of initial conditions. For the case under consideration, after some algebra and assuming a uniform distribution of initial conditions and a perfect adiabaticity of the process, which corresponds to neglecting the correction factor depending on  $K$  in  $c_{I \rightarrow III}$ ,  $c_{I \rightarrow II}$  and that the integral in Eq. (20) should be computed taking care of the sign of the  $\Theta_i$  in case of shrinking regions, then the estimate of  $\tau$  reads

$$\tau = \begin{cases} \frac{4\sqrt{1+\beta_f}}{\pi+4\sqrt{1+\beta_f}} & \text{for } -1 \leq \beta_f \leq \frac{\pi^2}{16} - 1, \\ \frac{4}{\pi} \sqrt{1+\beta_f} - \frac{1}{2} & \text{for } \frac{\pi^2}{16} - 1 \leq \beta_f \leq \frac{9\pi^2}{64} - 1, \\ 1 & \text{for } \beta_f \geq \frac{9\pi^2}{64} - 1. \end{cases} \quad (31)$$

This prediction is depicted as the solid line in Fig. 2.

We set up simulations with parameters identical to those described above, while  $T$  has been considered to be 30, 100, 3500 turns, respectively. The results of the numerical simulations are shown in Fig. 2 as series of markers of different colours for the different values of  $T$ . The agreement between the numerical simulations and the prediction improves as a

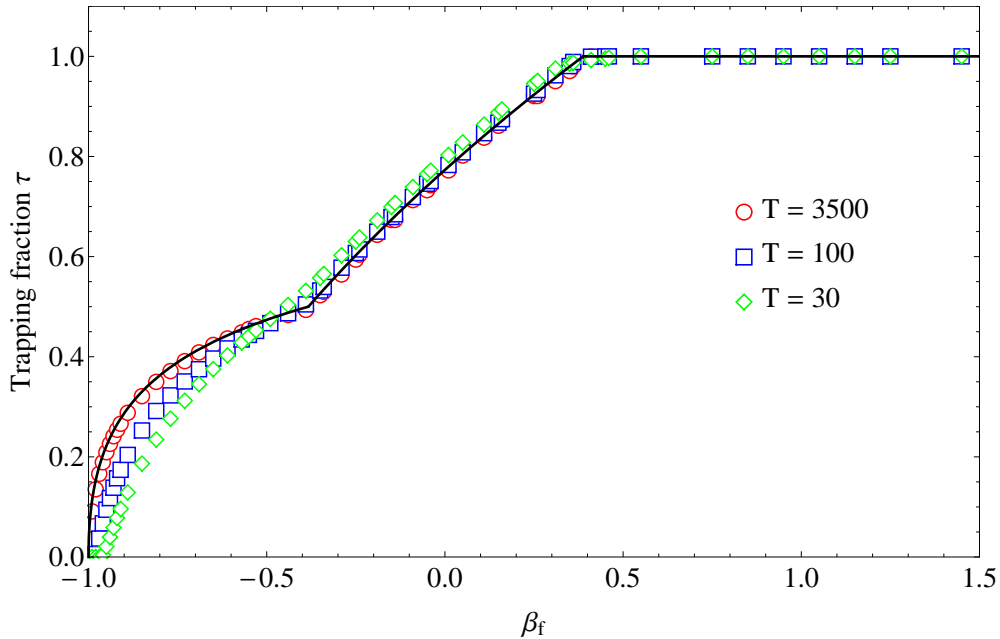


FIG. 2. The results of the trapping fraction study when we let  $\delta(\lambda)$  increase linearly while  $\beta(\lambda)$  increases quadratically. A close match with the results of the numerical simulations is visible for  $T = 3500$ .

function of  $T = 1/\epsilon$ . For shorter  $T$  the motion of the separatrix is not adiabatic and the trapping is shown to be less efficient in the part where  $\tau$  varies quadratically. However, when  $\tau$  varies linearly the trapping is even higher than the theoretical prediction. This might be due to the impact of the non-adiabaticity of the initial part of the trapping process that could have generated higher-density regions in the distribution, e.g., in the tails. This, in turn, could lead to an apparent increased trapping since in the theoretical model the particle distribution is assumed to be constant throughout the whole process.

## B. Optimisation of the trapping process

With the previous case, we showed that the theory is capable of describing the adiabatic trapping phenomenon with generic variation of the free parameters of the Hamiltonian (23). This opens up the possibility of performing an optimisation of the overall trapping process.

The first steps consist in exploiting the possibility of controlling independently the island position and its surface. This could lead to a fixed, but growing island, which would trivially trap all initial conditions intercepted by the expanding separatrix.

Another possibility consists in fixing the value of the  $\Theta_i$  in order to impose a well-defined trapping probability. Once more, the presence of two free parameters can be used for this purpose. It is easy to see that the phase space area beneath the stable island varies in time as

$$\Theta_{II} = 2\pi\dot{\delta} - \frac{\Theta_{III}}{2}. \quad (32)$$

Therefore, if  $\Theta_{II}$  is set to zero, then  $c_{I \rightarrow II}$  will be zero, too, thus providing a full trapping into Region *III*. The condition to impose is

$$\dot{\delta} = \frac{\Theta_{III}}{4\pi} = \frac{2\dot{\beta}(\lambda)}{\pi\sqrt{1+\beta(\lambda)}}. \quad (33)$$

Integrating with respect to  $\lambda$ , we find

$$\delta(\lambda) = \delta_0 + \frac{4}{\pi} \sqrt{1+\beta(\lambda)} \quad (34)$$

where we have assumed that  $\beta(0) = -1$ , corresponding to zero initial size for the island. This relation can also be inverted to give  $\beta(\lambda)$  with the required dependence on  $\delta(\lambda)$ :

$$\beta(\lambda) = \frac{\pi^2}{16} [\delta(\lambda) - \delta_0]^2 - 1. \quad (35)$$

It is worth noting that since the area of Region *II* remains constant, particles in that region must remain there since passing the separatrix would result in a decrease in the adiabatic invariant orbit-area. Therefore, under these conditions the trapping process will satisfy the following relations

$$N_{II} = N_{II}^0 \quad \text{and} \quad N_{III} = N_{III}^0 + N_I^0. \quad (36)$$

These considerations have been probed by a number of numerical simulations, whose results are presented in Fig. 3. The upper left plot refers to simulations performed with  $10^5$

initial conditions distributed uniformly over  $[-\pi, \pi] \times [2.2, 2.4]$  and where both  $\delta(\lambda), \beta(\lambda)$  vary linearly in time in such a way that both  $\Theta_{II}, \Theta_{III} > 0$ . The results are qualitatively as expected with particles in both Region *II* and *III*.

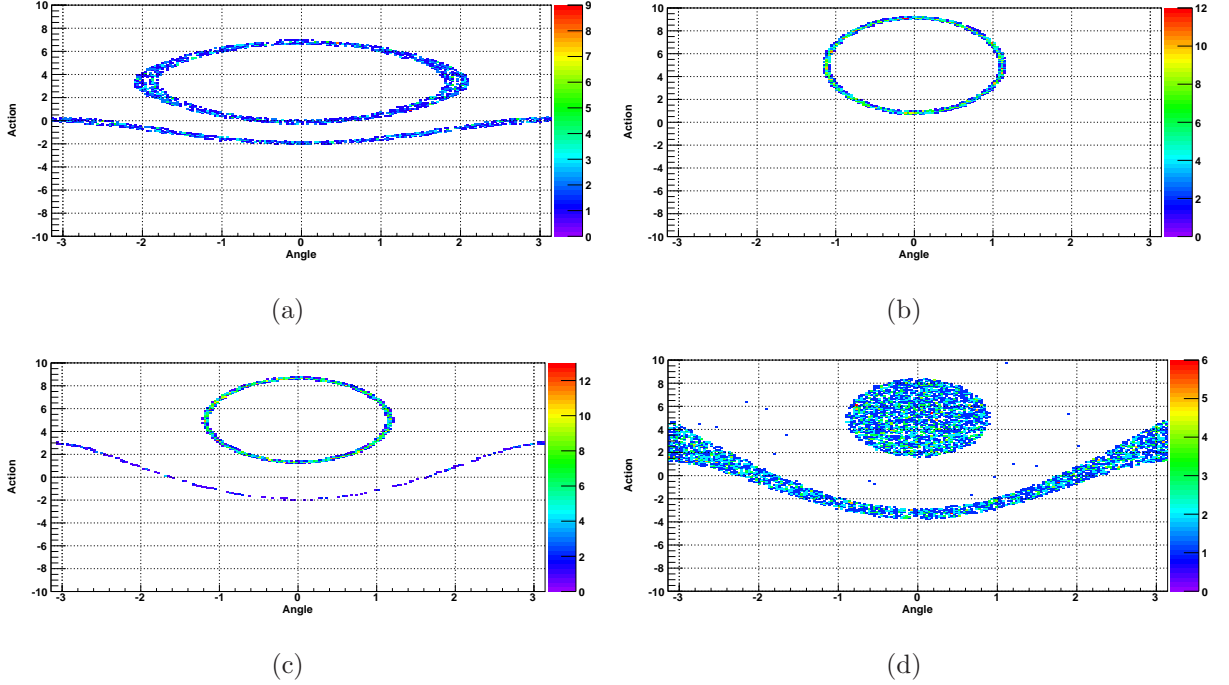


FIG. 3. Examples of final distributions generated from the same initial distribution and different relationships between  $\beta$  and  $\delta$  during the trapping process. (a): Transport of a growing island, obtained by a linear variation of both  $\delta(\lambda), \beta(\lambda)$ . (b): 100 % trapping into resonance obtained by using Eq. (35),  $\delta(\lambda) = 5\lambda/3000$ , and a resonance starting just below the initial distribution. (c): less than 100 % trapping into resonance obtained by using the same parameters as (b), but with  $\beta(\lambda)$  increasing more slowly, and a resonance starting just below the initial distribution. (d): 50 % trapping into resonance obtained by using the same parameters as (b), and a resonance starting in the middle of the initial distribution.

The remaining three plots refer to simulations with  $\delta(\lambda), \beta(\lambda)$  varying according to the relationship (35). Depending on where the island is created it is possible to share equally the initial conditions in Regions *II* and *III* (lower right plot of Fig. 3), or to have particles only in Region *III* (upper right plot). Finally, in the lower left plot a case in which  $\beta(\lambda)$  is varying more slowly than imposed by Eq. (35) is shown, which should simulate a non-optimal control of the system parameters. Of course, in this case some initial conditions are



trapped in Region *II*.

### C. Transport Efficiency

We were also interested in testing how efficiently a moving resonance can hold onto the particles undergoing libration around its point of stable equilibrium. This aspect is interesting as it could be combined with the trapping phenomena to transport towards higher values of  $I$  the conditions initially trapped into the islands. To this aim we define the transport efficiency  $\nu(\epsilon)$  as

$$\nu(\epsilon) = \frac{N_{III}^f}{N_{III}^i},$$

where  $N_{III}^i, N_{III}^f$  stand for the number of particles trapped in Region *III* at the beginning or at the end of the resonance transport, respectively. The theory predicts (see below) a simple power law should exist between the transport efficiency and the adiabatic parameter  $\epsilon/\omega_e^2$ .

To test this, we set up initial conditions for  $10^5$  particles in the rectangle  $[-\pi, \pi] \times [0, 1]$ , and let the stable island begin as a zero-size slit at  $I = 1/2$ . Then we let the island grow adiabatically until achieving a given area and thus capturing a given number of particles proportional to this area. Subsequently, we let the island move at various speeds by changing  $\delta$  from  $1/2$  to  $3$ .

The results, for many different final island sizes  $\Sigma_{III} \in [0, 2\pi]$  and various moving speeds (represented by the adiabatic parameter in the plot) are displayed in Fig. 4 and, fitting the regions between 10% and 60% efficiency, in order to probe the regime where adiabatic theory applies, a simple power law is found:

$$1 - \nu = (1.132 \pm 0.004) \left( \frac{\epsilon}{\omega_e^2} \right)^{0.754 \pm 0.003}. \quad (37)$$

It is interesting to investigate how the losses are distributed during the transport part of the process. The simulation results are shown in Fig. 5 where the losses as a function of turn number are depicted for several values of the adiabatic parameter. It is clearly seen that they occur at the very beginning of the transport stage, thus implying that only the trapped particles close to the separatrix are lost during the transport stage.

The scaling law found is understood in terms of the scaling provided by the theory based on the estimate of the trapping efficiency. Indeed, the time-distribution of the losses indicates

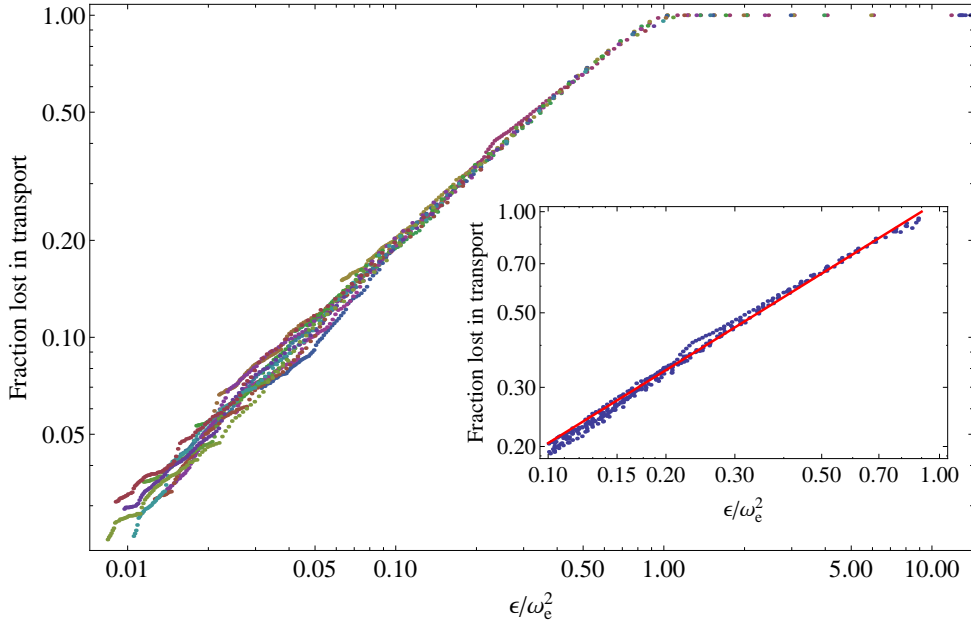


FIG. 4. Transport efficiency results after an island, full of particles in ligation, moves at various speeds. The theoretical prediction of a power-law dependence on the adiabatic parameter is confirmed.

that only the fraction of conditions that are in the region where the theory does not apply are eventually lost and no mechanism of re-filling such a region is acting during the whole process. Therefore, we need to estimate the phase space area corresponding to  $\Delta E \propto \epsilon^{3/2}$ .

To justify this scaling law we refer to the pendulum-like Hamiltonian (23): let  $\Delta\theta$  represent the change of  $\theta$  along the section  $I = \delta(\lambda)$ . The area  $\mathcal{A}$  in phase space where the validity of adiabatic theory fails turns out to be  $\mathcal{A} \propto L_{\text{sep}} \Delta\theta$ , where  $L_{\text{sep}}$  is the length of the separatrix. For  $\Delta\theta \ll 1$  we have  $\cos^2(\pi - \Delta\theta/2) \simeq \Delta\theta^2/4$  and consequently, given the relation between  $\Delta E$  and  $\Delta\theta$ , one obtains that  $\mathcal{A} \propto \epsilon^{3/4}$ . It is clear that for a uniformly distributed ensemble of particles  $\mathcal{A}$  is proportional to the number of particles that cannot be trapped in the resonance area during its translation in the phase space and this explains the result of numerical simulations, i.e., the exponent in Eq. (37).

In terms of control of the adiabatic trapping and transport, this result suggests that the strategy of separating the process into two well-distinct phases might not be the best option. In fact, the possible advantage of generating a growing but standing island in terms of trapping efficiency might be lost due to the losses appearing during the separate transport

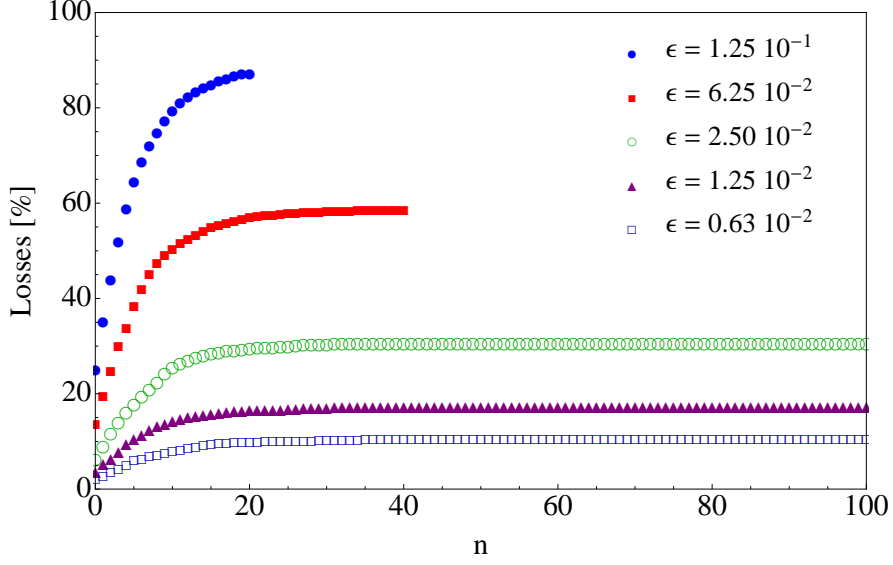


FIG. 5. Time-evolution of the losses during the transport stage of the process under study.

stage.

#### IV. ADIABATIC TRAPPING FOR AREA-PRESERVING MAPS

The second class of models under consideration is a generalisation of the quadratic polynomial 2D map, the so-called Hénon map [21]. The map reads

$$\begin{pmatrix} q \\ p \end{pmatrix}_{n+1} = R(\omega) \begin{pmatrix} q \\ p + q^2 + \kappa q^3 \end{pmatrix}_n \quad (38)$$

where  $R(\omega)$  is a 2D rotation matrix of an angle  $\omega$  and  $\kappa \in \mathbb{R}$ .

The corresponding interpolating Hamiltonian [22] is of the form (6), which, specialised to the case of the fourth-order resonance ( $m = 4$ ), reads

$$H(\psi, \rho, \lambda) = \lambda \rho + \frac{\omega_2(\lambda)}{2} \rho^2 + \lambda |u_{0,3}(\lambda)| \rho^2 \cos 4\psi, \quad (39)$$

in which

$$\omega_2(\lambda) = -\frac{1}{16} \left[ 3 \cot \frac{\omega(\lambda)}{2} + \cot \frac{3\omega(\lambda)}{2} + 6\kappa \right] \quad (40)$$

and

$$u_{0,3}(\lambda) = \frac{1}{16} \left[ \cot \frac{\omega(\lambda)}{2} - \cot \frac{3\omega(\lambda)}{2} - 2\kappa \right], \quad (41)$$

with

$$\omega(\lambda) = \lambda + \frac{\pi}{2} \quad \lambda = \frac{\Delta\omega}{T}t. \quad (42)$$

The fixed points satisfy the following conditions

$$\rho_+(\lambda) = -\frac{\lambda}{\omega_2(\lambda) + 2|u_{0,3}(\lambda)|\lambda} \quad \text{and} \quad \psi_+ = k\frac{\pi}{2} \quad (43)$$

or

$$\rho_-(\lambda) = -\frac{\lambda}{\omega_2(\lambda) - 2|u_{0,3}(\lambda)|\lambda} \quad \text{and} \quad \psi_- = \frac{\pi}{4} + k\frac{\pi}{2}. \quad (44)$$

Since the coordinate  $\rho$  is non-negative, we see that for the fixed points to exist we need the condition  $\lambda\omega_2(\lambda) < 0$ . Furthermore, the stability analysis shows that the fixed points  $(\psi_+, \rho_+)$  are stable while the  $(\psi_-, \rho_-)$  are unstable.

The separatrices have the form

$$\rho_{\text{sep}}^{\pm}(\lambda, \psi) = \frac{-\lambda \pm 2\sqrt{\frac{|u_{0,3}(\lambda)|\lambda^3 \cos^2 2\psi}{2|u_{0,3}(\lambda)|\lambda - \omega_2(\lambda)}}}{\omega_2(\lambda) + 2|u_{0,3}(\lambda)|\lambda \cos 4\psi} \quad (45)$$

and the surface of one island out of the chain of four is given by

$$\Sigma_{III} = 2\sqrt{\frac{\lambda^2}{4\lambda^2|u_{0,3}(\lambda)|^2 - \omega_2^2(\lambda)}} \tanh^{-1} \sqrt{\frac{4\lambda|u_{0,3}(\lambda)|}{\omega_2(\lambda) + 2\lambda|u_{0,3}(\lambda)|}}. \quad (46)$$

Finally, the angular frequency of oscillations around the elliptic fixed points is equal to

$$\omega_e(\lambda) = 4\lambda \sqrt{\left| \frac{\lambda u_{0,3}(\lambda)}{\omega_2(\lambda)} \right|}. \quad (47)$$

This model is more complex than the pendulum-like model. First of all some symmetries are lost, as is the case for the separatrices. In fact, the lower and upper separatrix branches are not symmetric anymore. Furthermore, the fact that all the coefficients of the Hamiltonian (6) are  $\lambda$ -dependent implies that this parameter affects both the position and the size of the island. A possibility to overcome this difficulty would be to use the additional free parameter  $\kappa$  as an additional tuning knob, making it a function of  $\lambda$ . This option has not been considered, yet.

The main features of the trapping process can be seen in Fig. 6. The initial conditions have been identified on the basis of the location at the end of the trapping process. It is clearly seen that the islands start trapping only at a finite distance from the origin. Then,

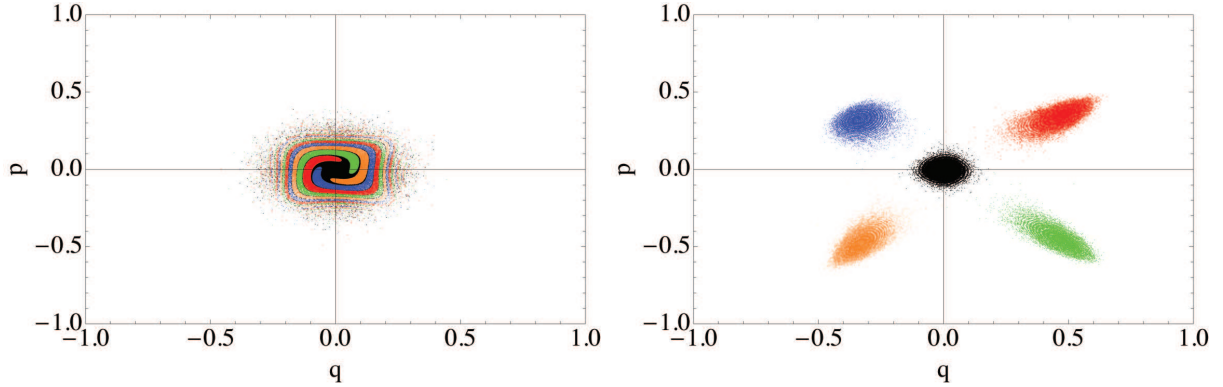


FIG. 6. Details of the trapping phenomenon for the map (38) with  $\kappa = -1.1$ ,  $\Delta\omega/T \approx 4.4 \times 10^{-6}$ , and a Gaussian initial distribution of  $5 \times 10^5$  particles with  $\sigma = 0.1$ . The initial conditions (left) have been coloured in order to identify in which island they will eventually be trapped (right).

in a given amplitude interval a well-defined area in phase space is trapped in the islands. At even larger amplitudes, a chaotic region appears and initial conditions arbitrarily close can end up in different islands.

The numerical studies aimed at probing the quantitative aspects of the trapping efficiency and of the scaling law of the no-trapping area around the origin.

### A. Analysis of $R_{\min}$

It is clear that  $R_{\min}$  is essential for any application aiming at a well-defined sharing of particles between islands and core. Simulations have been performed by using a uniform distribution of initial conditions and determining the fraction of trapped particles as a function of the radius  $R$  of the initial distribution. A fine scan over  $R$  has been performed, together with a fit of the computed trapping fraction to estimate its zero-crossing, which corresponds to  $R_{\min}$ . This procedure has been repeated for several values of  $T$  and the resulting  $R_{\min} = R_{\min}(T)$  are shown in Fig. 7 together with fit functions based on the scaling (16) for several values of the parameter  $\kappa$  and also resonance order  $m$ . The log-log plot shows an excellent agreement between the scaling law and the numerical results.

Additional numerical tests have been performed using unstable resonances, namely the  $1/3$  and the  $1/4$ . Indeed, while the first is generically unstable [22], the latter can be either stable or unstable. In our case, a modified version of the map (38) has been used,

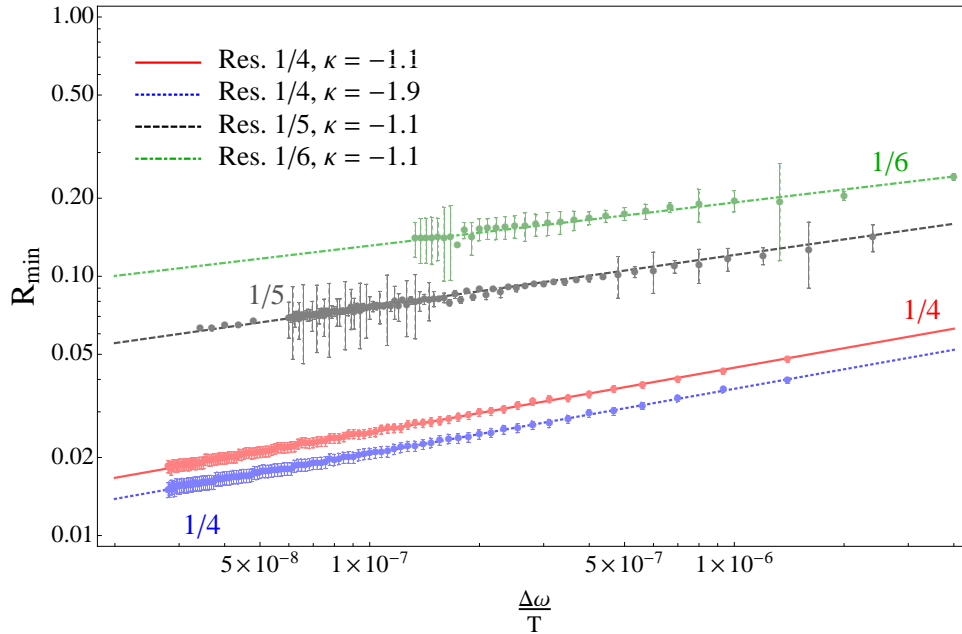


FIG. 7.  $R_{\min}$  as a function of the adiabatic parameter  $\Delta\omega/T$  in log-log scale. Different stable resonances and values of the parameter  $\kappa$  are shown together with the fit functions in which the exponents have been fixed according to the theory. The agreement with the proposed scaling law  $a(\Delta\omega/T)^{1/m}$  is remarkable.

where the parameters controlling the strength of the non-linear terms have been used to set  $\omega_2(\lambda) = 0$  in the Hamiltonian (6), which corresponds to turning the origin unstable, as described in Ref. [34]. In this case the control parameter  $\lambda$  has been changed in order to shrink the separatrix down to the origin, which is possible due to the unstable character of the resonance. Hence, the trapping process is somewhat different from the one considered so far. An example of the phase space topology for the  $m = 4$  stable and unstable resonance is shown in Fig. 8.

The results of the numerical simulations for the computation of  $R_{\min}$  are shown in Fig. 9. This scaling law agrees with the theoretical prediction given by the equation (18).

The summary of the fit parameters for both stable and unstable resonances is given in Table I for the fit functions  $a/T^b$ . In the case of the stable 1/4 resonance it has been possible to derive a scaling law for the parameter  $a$  of the fit, which is  $a(\kappa) = a_0 + a_1 \kappa$  with  $a_0 = 0.3 \pm 0.1$ ,  $a_1 = 1.6 \pm 0.2$  obtained by analysing numerical simulations for  $-1.9 \leq \kappa \leq -1.1$

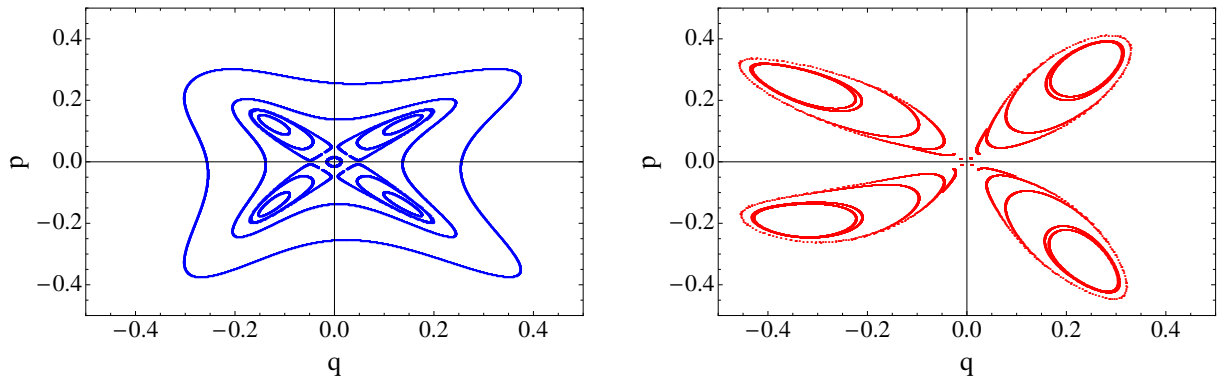


FIG. 8. Example of phase space portraits for the map (38) close to the stable resonance with  $m = 4$  (left) and its unstable version (right) based on the approach described in [34].

TABLE I. Summary of the fit parameters of the scaling law  $a/T^b$  for the evolution of  $R_{\min}$ .

Stability type	Resonance order	$\kappa$	$a \pm \Delta a$	$b \pm \Delta b$
stable	1/4	-1.1	$1.31 \pm 0.08$	$0.246 \pm 0.003$
stable	1/4	-1.9	$1.11 \pm 0.08$	$0.247 \pm 0.005$
stable	1/5	-1.1	$1.51 \pm 0.09$	$0.184 \pm 0.003$
stable	1/6	-1.1	$1.6 \pm 0.3$	$0.15 \pm 0.01$
unstable	1/3	-5.0	$3 \pm 1$	$0.48 \pm 0.01$
unstable	1/4	N.A.	$1.7 \pm 0.4$	$0.24 \pm 0.01$

in steps of 0.1.

### B. Analysis of trapping efficiency

Given the limited control over the topology of the phase space, the first item studied has been the behaviour of the trapping efficiency. A large campaign of numerical simulations has been performed, with the parameter  $\kappa$  scanned, as well as  $T$ . As far as the initial distribution is concerned, both Gaussian and uniform functions have been used, performing scans over their rms width.

The results of numerical simulations are reported in Fig. 10 (upper) where the trapping

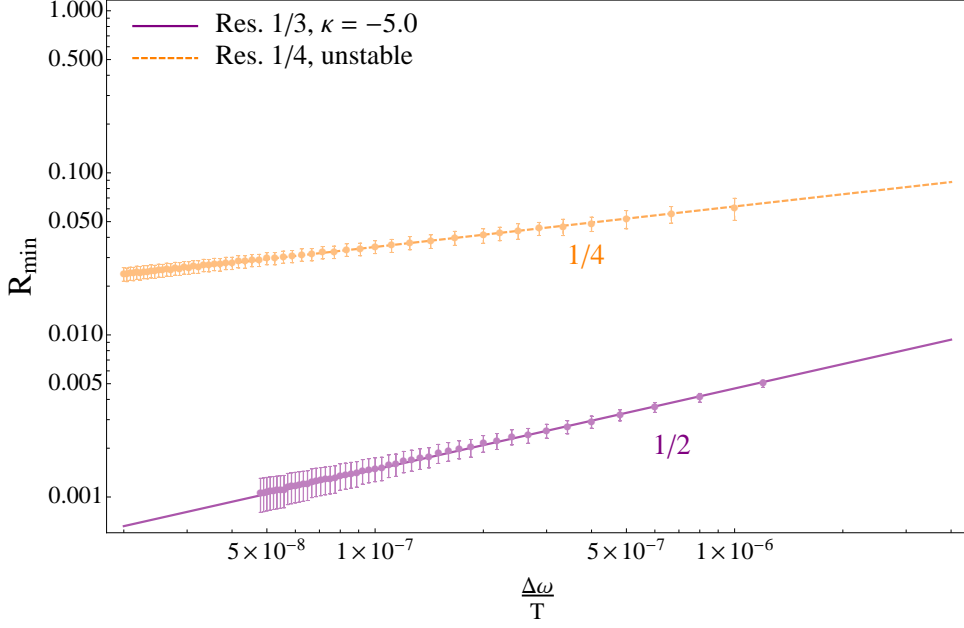


FIG. 9.  $R_{\min}$  as a function of the adiabatic parameter  $\Delta\omega/T$  in log-log scale. The 1/3 and 1/4 unstable resonances have been used. The exponents of the fit curves  $a(\Delta\omega/T)^b$  are shown in the plot. The agreement with the proposed scaling law  $a(\Delta\omega/T)^{1/2(m-2)}$  is remarkable.

fraction as a function of  $T$  is plotted for several values of the  $\sigma$  of the Gaussian distribution and for two values of  $\kappa$ . The numerical data have been fitted using the scaling law (21) and added to the plot as continuous lines. The agreement is remarkable and some discrepancy is visible only for the case referring to the smallest value of  $\sigma$ . It is important to point out that from the considerations of the previous section, where the quantity  $R_{\min}$  has been discussed, the lower limit of the integral (20) has been modified to take into account that no trapping can occur for amplitudes smaller than  $R_{\min}$ . Moreover, as  $R_{\min}$  depends on the adiabatic parameter, the trapping process will be affected differently as a function of  $T$ . Furthermore, as the value of  $\sigma$  becomes smaller, the impact of  $R_{\min}$  becomes larger; this explains why the agreement between the numerical data and the scaling law gets worse for small values of  $\sigma$ . Such an effect can be exactly quantified. The first step consists in computing the value  $\lambda_{\min}$  corresponding to  $R_{\min}$ , which is given by

$$2\pi R_{\min}^2 = \int_0^{2\pi} \rho_{\text{sep}}^+(\lambda_{\min}, \psi) d\psi. \quad (48)$$

As  $R_{\min} \ll 1$  it is possible to develop Eq. (48) and retain only the lower order term in  $\lambda_{\min}$ .



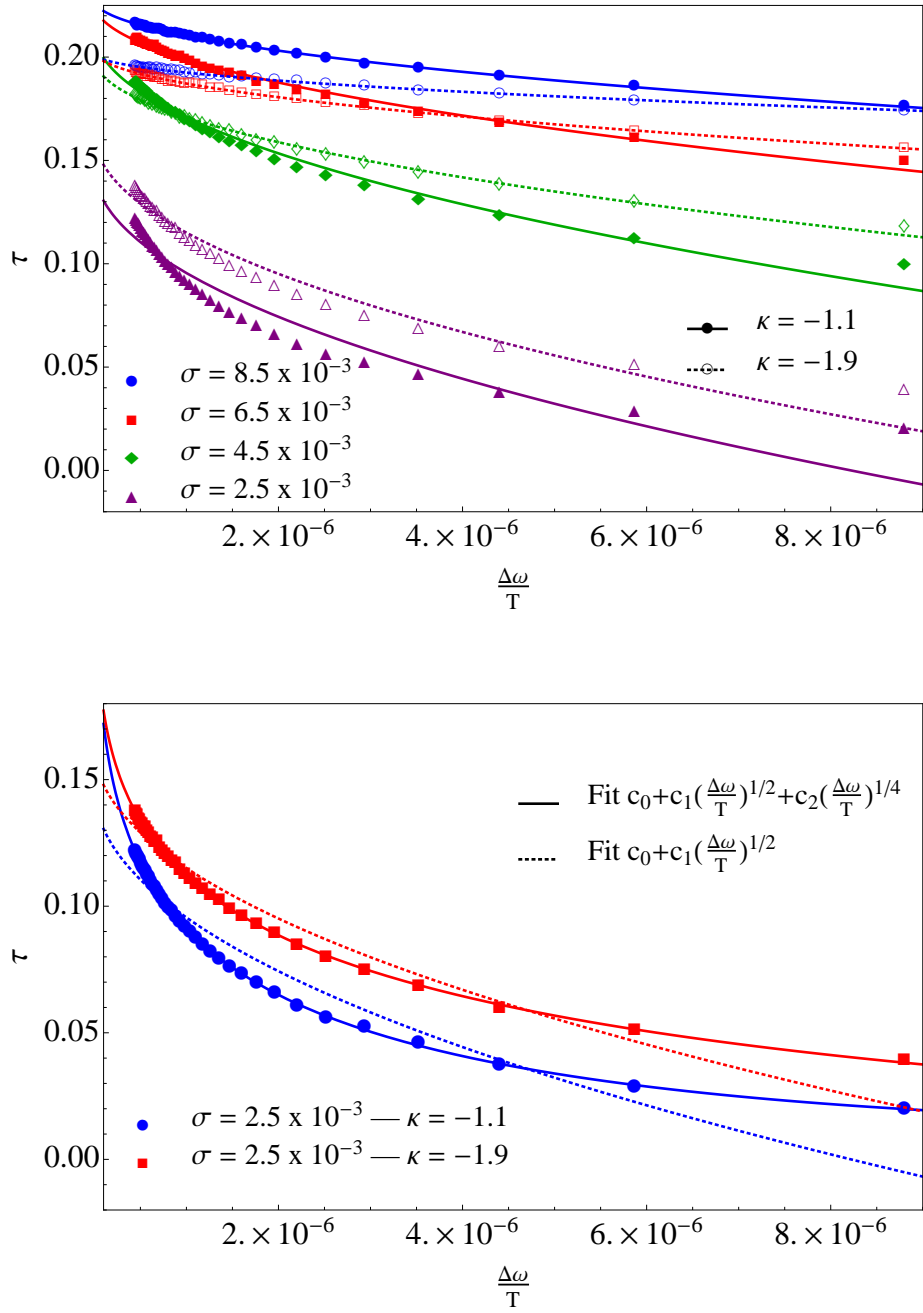


FIG. 10. Upper: Trapping fraction  $\tau$  (cf. Eq. (31)) as a function of the maximum number of iterations  $T$  for different values of  $\kappa$  and  $\sigma$  of Gaussian distributions. The fit curves are in very good agreement with the numerical data. Lower: Comparison of fit curves with and without the effect of  $R_{\min}$  for the simulations performed with smaller  $\sigma$ . The agreement is remarkable.

It is easy to show that

$$\lambda_{\min} \propto R_{\min}^2 \propto \epsilon^{2/m} \quad (49)$$

where the last step is valid in the case of stable resonances. The expression for  $N_{III}$  can be re-analysed by considering that in our simulations the lower limit of integration can be assumed to be zero, but the effect of  $R_{\min}$  has to be taken into account. Hence, Eq. (20) can be recast in the form

$$\begin{aligned} N_{III} &= \int_{\lambda_{\min}}^{\lambda_1} n(\rho(\lambda)) \frac{\Theta_{III}(\lambda)}{\Theta_I(\lambda)} \left[ 1 - 2K \frac{\sqrt{\epsilon}}{\omega_e(\lambda)} \right] d\lambda \\ &= \int_0^{\lambda_1} n(\rho(\lambda)) \frac{\Theta_{III}(\lambda)}{\Theta_I(\lambda)} \left[ 1 - 2K \frac{\sqrt{\epsilon}}{\omega_e(\lambda)} \right] d\lambda + \\ &\quad - \int_0^{\lambda_{\min}} n(\rho(\lambda)) \frac{\Theta_{III}(\lambda)}{\Theta_I(\lambda)} \left[ 1 - 2K \frac{\sqrt{\epsilon}}{\omega_e(\lambda)} \right] d\lambda \\ &\approx c_0 - c_1 \epsilon^{1/2} + c_2 \lambda_{\min} + c_3 \lambda_{\min}^{-1/2} \epsilon^{1/2} \\ &\approx c_0 - c_1 \epsilon^{1/2} + c_2 \epsilon^{1/2} + c_3 \epsilon^{1/2-1/m}. \end{aligned} \quad (50)$$

The term  $c_3 \lambda_{\min}^{-1/2} \epsilon^{1/2}$  is generated by the scaling  $\omega_e(\lambda) \approx \lambda^{-3/2}$  that can be derived from Eq. (47), while the last step of Eq. (50) is based on the estimate (49). In the particular case  $m = 4$  the scaling law for  $N_{III}$  simplifies to  $N_{III} \approx c_0 + c_1 \epsilon^{1/2} + c_2 \epsilon^{1/4}$ , with the re-definition of the symbols  $-c_1 + c_2 \rightarrow c_1$  and  $c_3 \rightarrow c_2$ . This prediction has been tested using the data referring to numerical simulations with the smaller  $\sigma$  shown in Fig. 10 (upper). The results are shown in Fig. 10 (lower). For the sake of comparison, the fit function obtained by neglecting the effect of  $R_{\min}$  is also shown. The improvement in the agreement between numerical data and theoretical prediction is clearly visible.

## V. CONCLUSIONS

In this paper we have shortly reviewed the theory of adiabatic trapping and transport for Hamiltonian systems and presented an extension suitable for applications to discrete-time systems, i.e., area-preserving modulated maps. We have explicitly considered two different classes of systems, namely a pendulum-like Hamiltonian and a Hénon map-like, to compare the analytical results with numerical simulations. The first class allows studying the parametric dependence of the trapping phenomenon, whereas by means of the second class we face the problem of extending the theoretical predictions to quasi-integrable discrete-time systems.

Our main goal is to understand the dependence of adiabatic trapping and transport efficiency on the system parameters, and to propose robust scaling laws suitable to be extended to more general models, relevant for physical applications.

Given the broad range of domains in which adiabatic trapping and transport play a crucial role, these results might be particularly relevant for applications. In particular, the results of these studies can be used in the process of optimising adiabatic transport or of mitigating the effects of unavoidable resonance crossing by proper control of the crossing process. It is worth stressing that these topics are of paramount importance, e.g., in the domain of particle accelerators, where novel beam manipulations have been proposed, based on adiabatic transport.

By means of extensive numerical simulations the scaling laws ruling the adiabatic transport and trapping have been verified and the agreement between predictions and numerical results is excellent. These laws allow us to understand and explore the domain of validity of the theory, which is essential to shed light on the detail of the trapping mechanism.

Even if these results have been obtained for rather generic systems, in terms of form of the underlying Hamiltonian, the dimensionality of the phase space is still too low and hence represents a limit to the applicability of our findings to realistic physical models. Therefore, the next step will be to attempt extending these results to Hamiltonian systems with two degrees of freedom where a richer phase space topology might lead to new phenomena.

## ACKNOWLEDGMENTS

We would like to thank J. Williams for useful comments on the original manuscript. One of the authors (AB) would like to thank the Accelerator and Beam Physics Group of CERN Beams Department for the hospitality.

## Appendix A: Adiabatic invariance for modulated area-preserving maps

To extend the adiabatic theory to the modulated map (3) we apply perturbation theory by introducing action-angle variables in each region defined by the separatrix curves. Let us define the generating function

$$F(q, E, \lambda) = \int_{H(q,p,\lambda)=E}^q p(\hat{q}, E, \lambda) d\hat{q} \quad (\text{A1})$$

where  $E = H(I, \lambda)$  is expressed as a function of the action variable

$$I(E, \lambda) = \frac{1}{2\pi} \oint_{H(q,p,\lambda)=E} p(q, E, \lambda) dq. \quad (\text{A2})$$

We perform the change of variables on the modulated map  $\mathcal{M}$  in (1) according to

$$\mathcal{N}(\epsilon n) = T^{-1}(\epsilon(n+1)) \circ \mathcal{M}(\epsilon n) \circ T(\epsilon n) \quad (\text{A3})$$

where the transformation  $T(\epsilon n) : (\theta_n, I_n) \rightarrow (q, p)$  is implicitly defined by

$$p = \left. \frac{\partial F}{\partial q} \right|_I (q, I_n, \epsilon n) \quad (\text{A4})$$

$$\theta_n = \left. \frac{\partial F}{\partial I} \right|_q (q, I_n, \epsilon n).$$

Remark: the variables  $(p, q)$  are uniquely defined whereas the definition of the variables  $(\theta_n, I_n)$  depends explicitly on  $n$  since the Hamiltonian function changes. According to our assumptions Eq. (A3) can be written in the form

$$\mathcal{N}(\epsilon n) = T^{-1}(\epsilon(n+1)) \circ T(\epsilon n) \circ \exp[D_{H(I, \epsilon n)}]$$

and we explicitly compute the map  $T^{-1}(\epsilon(n+1)) \circ T(\epsilon n)$  tangent to the identity from the relations

$$p = \frac{\partial F}{\partial q}(q, I_{n+1}, \epsilon(n+1)) = \frac{\partial F}{\partial q}(q, I_n, \epsilon n) + \epsilon \left. \frac{\partial}{\partial \lambda} \right|_{q,p} \frac{\partial F}{\partial q}(q, I_n, \epsilon n) + O(\epsilon^2) \quad (\text{A5})$$

$$\theta_{n+1} = \frac{\partial F}{\partial I}(q, I_{n+1}, \epsilon(n+1)) = \frac{\partial F}{\partial I}(q, I_n, \epsilon n) + \epsilon \left. \frac{\partial}{\partial \lambda} \right|_{q,p} \frac{\partial F}{\partial I}(q, I_n, \epsilon n) + O(\epsilon^2)$$

where  $I_n = I(q, p, \epsilon n)$  and, when not explicitly written, the partial derivatives are computed using  $F = F(q, I, \lambda)$ . From the definition (A4), algebraic calculations give

$$\frac{\partial^2 F}{\partial q \partial \lambda} + \frac{\partial^2 F}{\partial q \partial I} \frac{\partial I}{\partial \lambda} = 0 \quad (\text{A6})$$

$$\frac{\partial^2 F}{\partial I^2} + \frac{\partial^2 F}{\partial I \partial q} \frac{\partial q}{\partial I} = 0.$$

and from these relations we obtain

$$\begin{aligned} \left. \frac{\partial}{\partial \lambda} \right|_{q,p} \frac{\partial F}{\partial I} &= \frac{\partial^2 F}{\partial I \partial \lambda} + \frac{\partial^2 F}{\partial I^2} \frac{\partial I}{\partial \lambda} \\ &= \frac{\partial^2 F}{\partial I \partial \lambda} + \frac{\partial^2 F}{\partial q \partial \lambda} \frac{\partial q}{\partial I} = \left. \frac{\partial}{\partial I} \right|_{\theta} \frac{\partial F}{\partial \lambda}. \end{aligned} \quad (\text{A7})$$

The second equation of the system (A4) reads

$$\theta' = \theta + \epsilon \left. \frac{\partial}{\partial I} \right|_{\theta} \frac{\partial F}{\partial \lambda} + O(\epsilon^2),$$

where we identify  $\theta' = \theta_{n+1}$  and  $I = I_n$ . Finally, the map  $T^{-1}(\epsilon(n+1)) \circ T(\epsilon n)$  can be obtained by imposing the symplecticity conditions

$$\theta' = \theta + \epsilon \left. \frac{\partial}{\partial I} \right|_{\theta} \frac{\partial F}{\partial \lambda} + O(\epsilon^2)$$

$$I' = I - \epsilon \left. \frac{\partial}{\partial \theta} \right|_I \frac{\partial F}{\partial \lambda} + O(\epsilon^2)$$

(A8)

and is related to the phase flow at time  $\epsilon$  of the Hamiltonian

$$H_1(\theta, I, \lambda) = \frac{\partial F}{\partial \lambda}(q(\theta, I, \lambda), I, \lambda). \quad (\text{A9})$$

As a consequence, in the action-angle variables the modulated map (1) can be written in the form (3). Such map can be represented as a shift along trajectories of a two-frequency system [35] and the theory for two-frequency systems is applicable for this map. To prove the adiabatic invariance of the action  $I$  we apply a perturbative approach that introduces new action-angle variables  $(\phi, J)$

$$\theta = \phi + \epsilon \frac{\partial G}{\partial J}(\phi, J, \lambda) + O(\epsilon^2)$$

(A10)

$$I = J + \epsilon \frac{\partial G}{\partial \phi}(\phi, J, \lambda) + O(\epsilon^2)$$

to reduce the map (3) to an integrable form up to terms of order  $O(\epsilon^2)$ . By changing variables we obtain a homological equation to define  $G(\phi, J)$ :

$$G(\phi, J, \lambda) - G(\phi - \Omega(J, \lambda), J, \lambda) = H_1(\phi, J, \lambda), \quad (\text{A11})$$

where  $\Omega(J, \lambda) = \partial H(J, \lambda) / \partial J$ . According to [3] the following equality holds

$$\left. \frac{\partial F}{\partial \lambda} \right|_{q, I}(\theta, I) = -\frac{1}{\Omega(E, \lambda)} \int^{\theta} \left( \left. \frac{\partial H}{\partial \lambda} \right|_{q, p} - \left\langle \left. \frac{\partial H}{\partial \lambda} \right|_{q, p} \right\rangle \right) d\theta$$

where  $\langle \rangle$  is the average value with respect to the angle variable. Then one can prove

$$\left\langle \left. \frac{\partial F}{\partial \lambda} \right|_{q, I}(I, \theta) \right\rangle = 0 \quad (\text{A12})$$

and using the Fourier expansion

$$\frac{\partial H}{\partial \lambda} \Big|_{q,p} - \left\langle \frac{\partial H}{\partial \lambda} \Big|_{q,p} \right\rangle = \sum_{k \neq 0} h_k(I, \lambda) e^{i k \theta} \quad (\text{A13})$$

one computes

$$\frac{\partial F}{\partial \lambda} \Big|_{q,I}(I, \theta) = - \sum_{k \neq 0} h_k(I, \lambda) \frac{e^{i k \theta}}{i k \Omega(I, \lambda)}. \quad (\text{A14})$$

Then if  $\Omega(J, \lambda) \neq 0$  we get a formal solution of Eq. (A11) as

$$G(\phi, J, \lambda) = \sum_{k \neq 0} \frac{h_k(J, \lambda) e^{i k \phi}}{i k \Omega(J, \lambda) (1 - \exp[-i k \Omega(J, \lambda)]). \quad (\text{A15})$$

Remark: if we introduce the operator

$$\mathbb{T}_\Omega \sum_{k \neq 0} h_k(I, \lambda) e^{i k \theta} = \sum_k \frac{i k \Omega(I, \lambda)}{1 - \exp[-i k \Omega(I, \lambda)]} h_k(J, \lambda) e^{i k \theta} \quad (\text{A16})$$

and the new Hamiltonian

$$\hat{H}_1(\theta, I, \lambda) = \mathbb{T}_\Omega \frac{\partial F}{\partial \lambda}(\theta, I, \lambda) \quad (\text{A17})$$

the function  $G(\phi, J, \lambda)$  satisfies the homological equation

$$\Omega(J, \lambda) \frac{\partial G}{\partial \phi}(\phi, J, \lambda) = -\hat{H}_1(\phi, J, \lambda)$$

corresponding to the perturbation theory for Hamiltonian systems. This remark is useful to extend the adiabatic theory to slowly modulated area-preserving maps. The operator  $\mathbb{T}_\Omega$  changes the  $\theta$  Fourier components and its kernel is the average value. Moreover the following limit holds [for any finite and fixed  \$k\$](#)

$$\lim_{\Omega \rightarrow 0} \frac{i k \Omega(I, \lambda)}{1 - \exp[-i k \Omega(I, \lambda)]} = 1.$$

Since the frequency  $\Omega(I, \lambda)$  vanishes at the separatrix curve, the operator  $\mathbb{T}_\Omega$  can be extended up to the separatrix curve [if one considers finite Fourier series](#). However, the operator  $\mathbb{T}_\Omega$  is defined in an open set of the action variable if there are no resonance conditions (5) for each Fourier component  $k$  in the expansion (A15).

Therefore, a cut-off  $k_{\max}$  has to be introduced in the Fourier expansion (A15) and it should be proved that the remainder is of order  $O(\epsilon)$ . [To this aim it is customary to extend the domain of definition of  \$\theta\$  to the complex plane, in order to make use of the estimates](#)

available for analytic functions in  $\mathbb{C}$ . Assuming that  $\partial H/\partial\lambda$  is a bounded analytic function in a strip  $|\text{Im } \theta| \leq \gamma(I, \lambda)$  such as for a given action value  $I$

$$\left| \frac{\partial H}{\partial \lambda} \Big|_{q,p} \right| \leq M$$

with  $M$  a constant independent from  $I$ , then following estimate holds [36]

$$\begin{aligned} \sum_{|k| \geq k_{\max}} \frac{|h_k(I, \lambda)|}{k \Omega(I, \lambda)} &\leq e^{-\gamma(I, \lambda) k_{\max}} \sqrt{\sum_{|k| \geq k_{\max}} |h_k(I, \lambda)|^2 e^{2\gamma(I, \lambda) |k|}} \sqrt{\sum_{|k| \geq k_{\max}} \frac{1}{[k \Omega(I, \lambda)]^2}} \\ &\leq c \frac{e^{-\gamma(I, \lambda) k_{\max}}}{k_{\max} \Omega(I, \lambda)} M \end{aligned} \quad (\text{A18})$$

taking into account the cut-off  $k_{\max}$  in the Fourier expansion. Then, by solving the homological equation (A11) neglecting the Fourier components  $|k| \geq k_{\max}$  the remainder is of order  $O(\epsilon)$  provided  $k_{\max}$  fulfils the condition

$$\frac{c M e^{-\gamma(I, \lambda) k_{\max}}}{k_{\max} \Omega(I, \lambda)} \leq \epsilon. \quad (\text{A19})$$

We remark that  $k_{\max}$  is a function of  $I$  and  $\lambda$  so that it is defined locally in phase space.

From these considerations it is possible to cast the map (3) in the form (4). The further step consists in analysing the domain of validity of the cut-off introduced earlier.

Under generic assumptions the relation  $\phi = \Omega t$  suggests the estimate  $\gamma(I, \lambda) \simeq \gamma_0 |\Omega(I, \lambda)|$ . Furthermore, one expects that  $\gamma_0^{-1}$  can be related to  $\max |\Omega(J, \lambda)|$  in the considered phase space region. From the inequality (A19), we obtain the condition

$$k_{\max} |\Omega(I, \lambda)| \geq \chi(\gamma_0, M, \epsilon) \quad \text{where} \quad \epsilon = \frac{c M e^{-\gamma_0 \chi}}{\chi}. \quad (\text{A20})$$

The small denominators  $1 - \exp[-k\Omega(J, \lambda)]$  in the expansion (A15) can be controlled if

$$k_{\max} |\Omega(J, \lambda)| \leq c' < 2\pi.$$

Comparing the constraints on  $k_{\max} \Omega$  we obtain a final condition on  $\gamma_0$  and  $M$  in the form:

$$\chi(\gamma_0, M, \epsilon) \leq c',$$

which is satisfied if

$$\epsilon \geq \frac{c M e^{-2\pi\gamma_0}}{2\pi}. \quad (\text{A21})$$

This implies that the adiabatic invariance of the action for such maps cannot hold for arbitrarily small values of  $\epsilon$  due to the presence of non-linear resonances. Nevertheless, once condition (A21) is satisfied, it can be applied in a neighbourhood of the separatrix curve since it holds in the limit  $\Omega \rightarrow 0$ ,  $k_{\max} \rightarrow \infty$  with  $k_{\max} \Omega \simeq \text{const}$ . Therefore, the function

$$J(\theta, I, \lambda) = I - \epsilon \sum_{\substack{|k| \leq k_{\max}(\Omega, \epsilon) \\ k \neq 0}} \frac{i k h_k(J, \lambda) e^{i k \theta}}{1 - \exp[-i k \Omega(J, \lambda)]} + O(\epsilon^2) \quad (\text{A22})$$

can be extended up to the separatrix curve in each phase space region. When approaching the separatrix ( $\Omega \rightarrow 0$ ) the function  $J(\theta, I, \lambda)$  tends to the IAI [37] of the interpolating Hamiltonian  $H(q, p, \lambda)$  that has been introduced in Eq. (2). Hence, once the condition (A21) is satisfied, the new map (4) implies that the action  $I$  is an adiabatic invariant for the initial dynamics (1) if we are not too close to the separatrix. By performing another perturbative step we can also prove that the new action  $J$  is an IAI if we restrict the condition (A21) to cut-off terms of order  $O(\epsilon^2)$ , i.e.

$$\epsilon \geq \sqrt{\frac{c M}{2 \pi}} e^{-\pi \gamma_0}. \quad (\text{A23})$$

Therefore, the application of the adiabatic invariance theory to analytic maps in a neighbourhood of an elliptic fixed point is justified for  $\epsilon$  values that satisfy the condition (A23).

---

## REFERENCES

- [1] A. Neishtadt, “Passage through resonances in the two-frequency problem”, *Sov. Phys. Dokl.*, **20**, 189, 1975.
- [2] A. Neishtadt, “Passage through a separatrix in a resonance problem with a slowly-varying parameter”, *J. Appl. Math. Mech.*, **39**, 594, 1976.
- [3] A. Neishtadt, “Change of an adiabatic invariant at a separatrix”, *Sov. J. Plasma Phys.*, **12**, 568, 1986.
- [4] J. L. Tennyson, J. R. Cary, and D. F. Escande, “Change of the Adiabatic Invariant due to Separatrix Crossing”, *Phys. Rev. Lett.* **56**, 2117, 1986.
- [5] J. R. Cary, D. F. Escande, and J. L. Tennyson, “Adiabatic-invariant change due to separatrix crossing”, *Phys. Rev. A* **34**, 4256, 1986.



- [6] B. V. Chirikov and V. V. Vecheslavov “Adiabatic Invariance and Separatrix: Single Separatrix Crossing”, *Journal of Experimental and Theoretical Physics*, **90-3**, 562, 2000.
- [7] B. V. Chirikov, “Particle confinement and adiabatic invariance”, *Proc. Royal Soc. London A* **413**, 145, 1987.
- [8] A. Neishtadt, A. A. Vasiliev and A. Itin, “Captures into resonance and scattering on resonance in dynamics of a charged relativistic particle in magnetic field and electrostatic wave”, *Physica D* **141**, 281, 2000.
- [9] R. Cappi, M. Giovannozzi, “Novel Method for Multiturn Extraction: Trapping Charged Particles in Islands of Phase Space”, *Phys. Rev. Lett.* **88**, 104801, 2002.
- [10] R. Cappi, M. Giovannozzi, “Multiturn extraction and injection by means of adiabatic capture in stable islands of phase space”, *Phys. Rev. ST Accel. Beams* **7**, 024001, 2004.
- [11] S. Gilardoni, M. Giovannozzi, M. Martini, E. Métral, P. Scaramuzzi, R. Steerenberg, and A.-S. Müller, “Experimental evidence of adiabatic splitting of charged particle beams using stable islands of transverse phase space”, *Phys. Rev. ST Accel. Beams* **9**, 104001, 2006.
- [12] A. Franchi, S. Gilardoni, and M. Giovannozzi, “Progresses in the studies of adiabatic splitting of charged particle beams by crossing nonlinear resonances”, *Phys. Rev. ST Accel. Beams* **12**, 014001, 2009.
- [13] A. Neishtadt, “Jumps in the adiabatic invariant on crossing the separatrix and the origin of the 3:1 Kirkwood gap”, *Sov. Phys. Dokl*, **32**, 571, 1987.
- [14] A. Neishtadt, “Scattering by resonances”, *Celestial Mechanics and Dynamical Astronomy*, **65**, 1, 1997.
- [15] S. Sridhart and J. Touma “Adiabatic evolution and capture into resonance: vertical heating of a growing stellar disc”, *Mon. Not. R. Astron. Soc.* **279**, 1263, 1996.
- [16] Q. Niu, “Quantum adiabatic particle transport”, *Phys. Rev. B* **34**, 5093, 1986.
- [17] O. Entin-Wohlman, A. Aharony, and Y. Levinson, “Adiabatic transport in nanostructures”, *Phys. Rev. B* **65**, 195411, 2002.
- [18] J. P. Pekola, J. J. Toppari, M. Aunola, M. T. Savolainen, and D. V. Averin, “Adiabatic transport of Cooper pairs in arrays of Josephson junctions”, *Phys. Rev. B* **60**, R9931, 1999.
- [19] V. I. Arnol’d, “Conditions of the applicability and an estimate of the mistake of the averaging method for systems, which goes through the resonances during the evolution process”, *Doklady*, **161**, 9, 1965.

- [20] V. Arnol'd, V. Kozlov, A. Neishtadt, *Mathematical Aspects of Classical and Celestial Mechanics*, Springer, 2006.
- [21] M. Hénon, “Numerical study of quadratic area-preserving mappings”, *Q. Appl. Math.* **27**, 291, 1969.
- [22] A. Bazzani G. Servizi, E. Todesco, G. Turchetti, “A Normal Form Approach to the Theory of Nonlinear Betatronic Motion”, CERN Yellow Report 94-02, 1994.
- [23] A. Bazzani, S. Marmi, G. Turchetti, “Nekhoroshev estimate for isochronous non resonant symplectic maps”, *Celestial Mechanics and Dynamical Astronomy* **47**, 333, 1990.
- [24] G. D. Birkhoff, “Surface transformations and their dynamical applications”, *Acta Math.* **43**, 1, 1920.
- [25] A. Bazzani, M. Giovannozzi, G. Servizi, E. Todesco and G. Turchetti, “Resonant normal forms, interpolating hamiltonians and stability analysis of area preserving maps”, *Physica D* **64** 66, 1993.
- [26] A. Bazzani, F. Brini, G. Turchetti, “Diffusion of the Adiabatic Invariant for Modulated Symplectic Maps”, *AIP Conf. Proc.* 395, 129, 1997.
- [27] A. Bazzani, F. Brini, “Modulated Diffusion for Symplectic Maps”, in *Hamiltonian Systems with Three or More Degrees of Freedom*, NATO ASI Series Volume 533, 300, 1999.
- [28] D. L. Bruhwiler, J. R. Cary, “Diffusion of particles in a slowly modulated wave”, *Physica D*, **40**, 265, 1989.
- [29] M. Aiba, S. Machida, Y. Mori, and S. Ohnuma, “Resonance crossing experiment at a proof of principle fixed field alternating gradient accelerator”, *Phys. Rev. ST Accel. Beams* **9**, 084001, 2006.
- [30] M. Giovannozzi and J. Morel, “Principle and analysis of multiturn injection using stable islands of transverse phase space”, *Phys. Rev. ST Accel. Beams* **10**, 034001, 2007.
- [31] D. Vainchtein and I. Mezić, “Capture into Resonance: A Method for Efficient Control”, *Phys. Rev. Lett.* **93**, 084301, 2004.
- [32] A. Neishtadt, “Probability phenomena due to separatrix crossing”, *Chaos* **1**, 42, 1991.
- [33] A.I. Neishtadt, “On probabilistic phenomena in perturbed systems” in: Bazykin, A. (Ed.) *et al. Mathematics and Modelling* NTsBI Akad. Nauk SSSR, Pushchino (1990), 141, Engl. transl.: *Selecta Math. Sov.* **12-3**, 195, (1993).
- [34] M. Giovannozzi, D. Quatraro, and G. Turchetti, “Generating unstable resonances for extrac-

- tion schemes based on transverse splitting”, *Phys. Rev. ST Accel. Beams* **12**, 024003, 2009.
- [35] A. Neishtadt, “Capture into resonance and scattering on resonances in two-frequency systems”, *Proceedings of the Steklov Institute of Mathematics*, **250**, 183, 2005.
- [36] H. Rüssmann, “On optimal estimates for the solutions of linear difference equations on the circle”, *Celestial Mechanics and Dynamical Astronomy* **14**, 33, 1976.
- [37] V. I. Arnol’d, “On the behavior of adiabatic invariants under a slow periodic change of the Hamiltonian function”, *Doklady*, **142**, 758, 1962.